ENEL400

2013 Third Professional Year Project
Direct Drive Electric Scooter

Matthew L. Kokshoorn

Supervisor: Dr. Paul Gaynor

23rd August 2013

Abstract

This report details the design and development of a direct drive electric scooter, a 3rd professional year engineering project aiming to provide an alternative form of short range transport for urban areas. It discusses the mechanical design of a lithium iron phosphate battery housing component to be integrated into a children's scooter frame as well as the fabrication of a rim for fitting of a brushless direct current hub motor. It also covers the electrical and software development including the implementation of an overcurrent control procedure using an i^2t approach. The electrical design predominantly deals with the interfacing with a Golden Motor brushless direct current motor speed controller and the processing of user inputs. The design can be considered a success, achieving loaded speeds of 15 km/hr with an expected range of 20km and effectively limiting current to avoid thermal damage to the motor.

1. INTRODUCTION

Prior to this project the department was in possession of a brushless direct current (BLDC) motor speed controller (MSC), a BLDC hub motor, a number of lithium iron phosphate cells and a recently purchased children's scooter (see Figure 5). The objective of this project was to use these parts, along with others yet to be purchased, to design and build a fully functional direct drive electric scooter, complete with display interface, battery charge monitoring and an over current implementation to achieve a boost feature. An overview of the proposed system can be seen below in Figure 1 (see Appendix 1 for physical system locations). To ensure that the BLDC motor is protected from thermal damage in periods of 'over current' an i^2t algorithm was proposed.

In order to produce an effective product, considerable amounts electrical, mechanical and software designs were required. The mechanical portion included the design of a battery/motor-controller housing compartment and its integration to the scooter frame. Additionally, a new rim for fitting of a BLDC motor was designed. The electrical aspects concerned the design and implementation of two circuit boards. One for these boards, referred to as the primary board, was designed to contain a microprocessor to carryout overcurrent logic and relay data to a LCD display. The second board, referred to the as the secondary board, was designed to possess a current transducer and carry out signal conditioning within closer proximity the motor. The two boards are connected by a ribbon cable and designed to operate in a noisy environment. Finally the software design concerned the underlying system control strategy and the i^2t overcurrent algorithm.

The motivation behind the project is to provide an alternative form of short range transport for urban areas. A lot of commercially available electric scooters tend to be slow and inefficient. By utilizing the set of new generation lithium iron phosphate batteries and a BLDC hub motor, it is the aim to overcome some of these limitations. The batteries and motor are capable of high power densities (power/kg) and therefore make them ideal for light weight vehicles such as this. By using this technology, the aim is also to overcome some of the weight issues associated with other electric scooters and therefore improve the speed and efficiency.

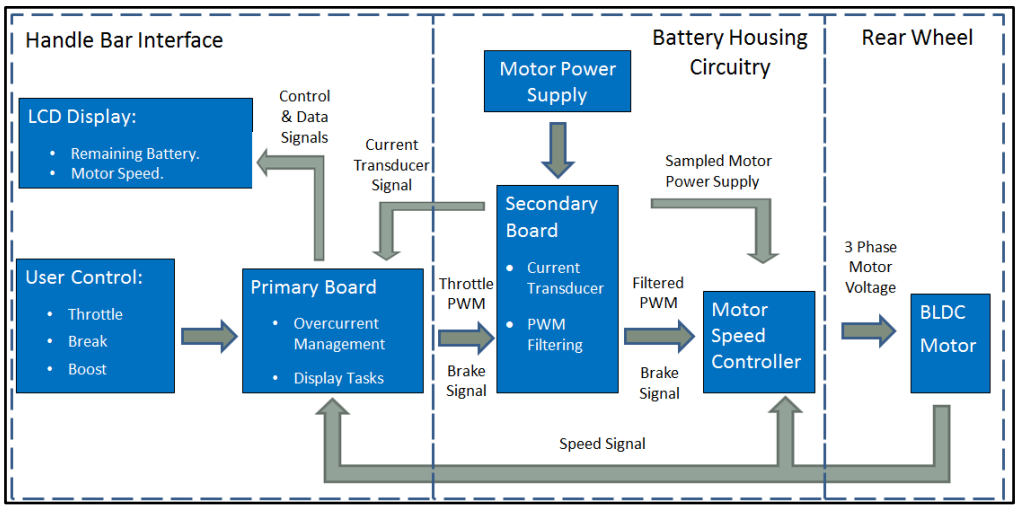

Figure 1 - Direct Drive Electric Scooter System Overview.

2. THEORY OF OPERATION

2.1 Brushless Direct Current Hub Motor

The BLDC hub motor used in this project uses an axial design with a side by side rotor and stator with an air gap separation. The inner stator potion of the motor is attached to the frame of the scooter, leaving outer rotor free to rotate (see Figure 2). In this project, the rotor is attached to a fabricated nylon rim (see section 3.1.2 - BLDC Hub Rim). The design also includes permanent magnets on the rotor providing the magnetic fields for the motor to generate torque.

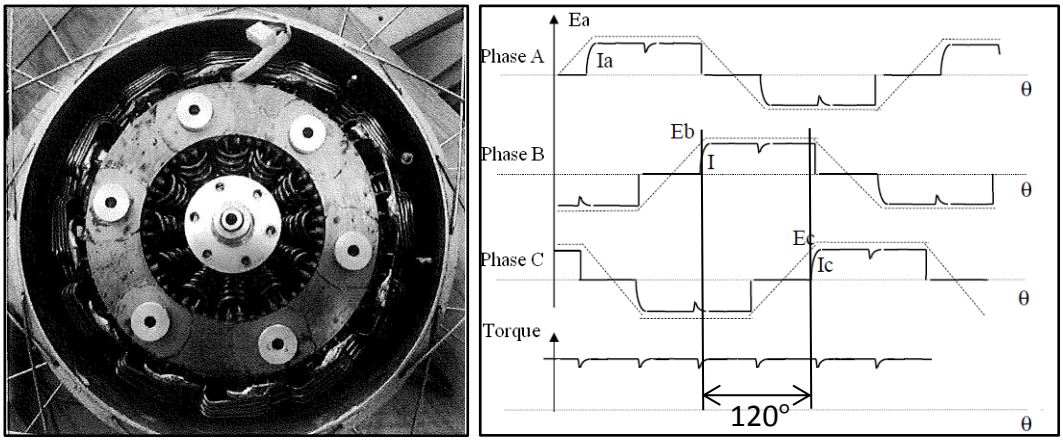

Figure 2 - Avanti Electra's BLDC Hub Motor [1] (Left) and Theoretical BLDC Three Phase Waveforms (Right) [2].

The motor operates in a similar manner to synchronous machines with exception that it uses permanent magnets on the rotor as opposed to electromagnets. A MSC inverts the DC supply to generate three trapezoidal AC signals each out of phase by 120 degrees as can be seen above in Figure 2. These three signals are then applied to the stator's electromagnets causing the machine's rotor to generate torque. Given this torque is greater than the machines mechanical load, it will give rise to rotational motion.

BLDC motors have a number of benefits over other electrical DC machines such as brushed DC motors. They require fewer mechanical parts and as such are subject to less wear and possess longer lifetimes. Additionally, owing to not having mechanical brushes, BLDC motors are typically easier to cool and generate less electrical noise [3]. Although BLDC motors typically have a higher initial cost, this can normally be recovered through efficiency and maintenance advantages. Part of this high initial cost is due to the requirement of a MSC to generate the three trapezoidal AC signals.

2.2 BLDC Motor Speed Controller

BLDC motors, although described as being DC machines, require a MSC to operate as invert the DC supply. The MSC requires some means of determining the position of the rotor relative to stator. In the context of this project this is done using six Hall Effect sensors evenly distributed every 60 degrees around the stator as can be seen in Figure 2. These sensors allow the MSC to determine the motor's position and direction of motion and thus apply the appropriate phase to each electromagnet to accelerate to a desired speed.

The BAC-0281 Golden Motor BLDC MSC used in this project is rated for 24V - 48V and capable of supplying up to 30A continuous current to the motor with a peak current of 50A [4]. It has a number of features including; regenerative braking, maximum speed limiting and reverse.

2.3 i^2t Overcurrent Algorithm

Motors are supplied with a nominal power/current rating so that their thermal capacity is not exceeded, causing damage to the machine. As a general rule, however, BLDC motors can be operated at twice their rated current for approximately one minute. To utilise this principal, while protecting the motor from exceeding its thermal capacity, a control strategy must be applied. For this project an i^2t tracking approach has been implemented. The approach essentially integrates the positive difference between the motor current squared and the current rating squared, when the motor current is exceeding the rated value (i.e. the tracking variable cannot go below zero). This is demonstrated below in Figure 3 with a system that is rated for 15A and abides by the limitation that it must not exceed the thermal equivalent of being run at double the rated current for three seconds .This i^2t limit is calculated as $90A^2s$ [5] by equation 1,

$$i^2t_{limit} = (2 \times I_{rated})^2 \times T_{rated} \tag{1}$$

where T_{rated} represents the time at double the rated current, I_{rated} . Figure 3 shows the i^2t tracking variable beginning to increase as the motor current rises above 15A ($t = 9s$). Once the i^2t limit has been met ($t = 17.3s$), the output current is dropped to 15A in order to prevent damage to the machine and ensure the i^2t limit is not exceeded. As the current begins to drop below the 15A($t = 24s$) rating, the i^2t tracking variable begins to decrease, allowing the motor current to once again exceed the rated current.

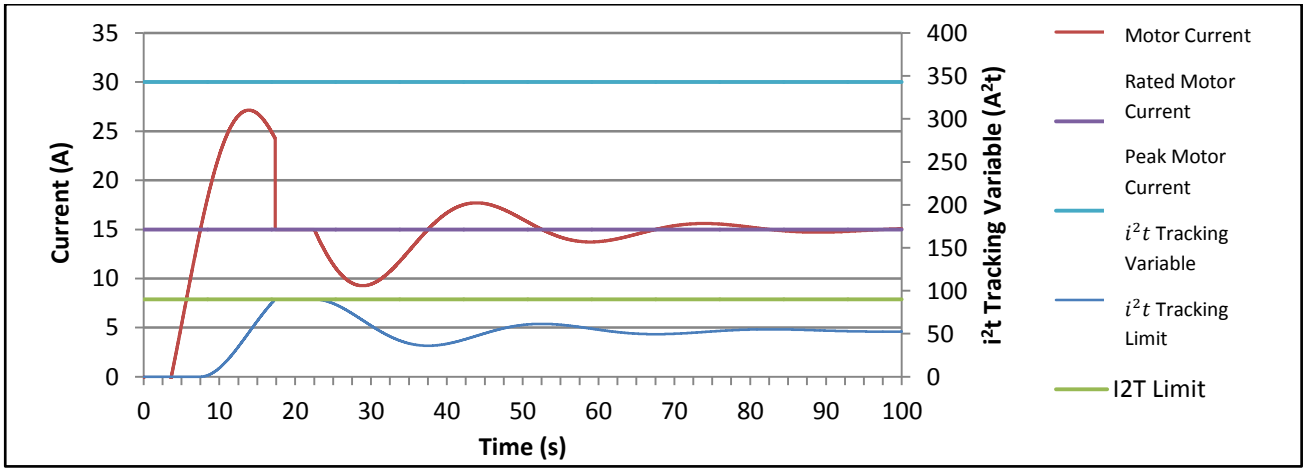

Figure 3 – Example System Demonstrating i^2t Tracking Algorithm.

This method is used over an $i \times t$ approach as it more accurately reflects the energy dissipated in the motor winding. This can be seen as thermal energy calcualted by equation 2,

$$E_d = P_d \times t = I_m^2 \times R_w \times t \tag{2}$$

where E_d and P_d represent the energy and power dissipated respectively, I_m represents the motor current and R_w represents the resistance of the motor armature windings.

2.4 Lithium Iron Phosphate Cells

Lithium Iron Phosphate ($LiFePO_3$) or Lithium Ferro Phosphate (LFP) cells are a type of rechargeable battery that offer high power density and long life times. A set of A123Systems ANR26650-M1 cells are used in this project (see Figure 4). They are considered safer than the more commercially common Lithium Cobalt Oxide ($LiCoO_2$) however do generally have a lower energy density. Due to the higher power density they are often found in electro-mechanical applications owing to the high discharge currents involved with acceleration. For this reason the cells are ideal for the scooter project, each weighing only 72g and occupying a space specified as a 26mm diameter of length 65mm. Each cell has a nominal voltage of 3.3V and is capable of a discharge current of 100A [6] . They each possess a total charge of 2.3Ahr and cost approximately $4.25 NZD each.

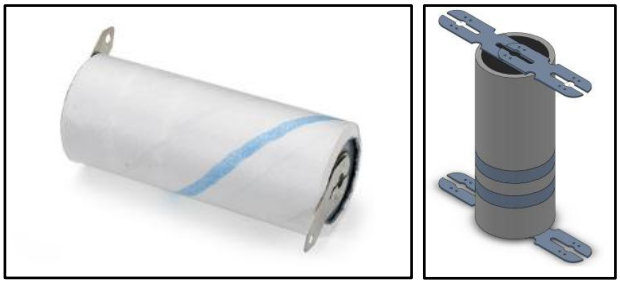

Figure 4 – LPF A123 System ANR26650-M1 Cell [7] Photo (Left) and Solid Works Model (Right).

2.5 Overall System Operation

By combining the theory previously discussed, the operation behind the direct drive electric scooter can be described. The final product (see Figure 5) is controlled by a microcontroller encased on the handle bars. It is in microcontroller where the i^2t tracking algorithm is implemented in software. From this logic, the motor speed is controlled by sending a variable voltage to the MSC located in the battery casing near the rear wheel. The MSC then generates the appropriate trapezoidal signals to bring the motor to this speed with position and speed feedback from the BLDC Hall Effect sensors. The system uses forty of the LFP cells previously (See section 2.4 - Lithium Iron Phosphate Cells) arranged as 8 series sets of 5 paralleled cells. This gives a supply voltage of 26.6V with a maximum current supply of 500A and energy capacity of 303.6 Whr. This gives an expected range of 20km based on an average speed of 10km/hr at 150W.

Figure 5 - Unmodified Children's Scooter (Left) and Final Direct Drive Electric Scooter (Right).

3. DISCUSSION

The engineering design process applied to the design of the scooter called for three concurrent streams of development. The first of these was the mechanical design, concerning with the fitting of the BLDC motor itself, the battery housing design and its integration with the scooter frame. The second was the electrical design concerning the primary and secondary board design, their population and their testing. Finally the third stream of development involved the software design, made concurrent by the use of a developer's board. The subsequent sections discus the design decisions and problems associated with each of these streams.

3.1 Mechanical Design and Overall Configuration

3.1.1 Battery/Motor-Controller Housing

The housing component of the scooter had to be designed to hold forty LFP cells and the Golden Motor MSC. In order to accurately carry out this design, the cells and scooter frame were modelled using solid works and a casing component modelled around this to meet the correct dimensions with sufficient clearances for wiring. The initial design did not incorporate the MSC and can be seen in Appendix 15 and Appendix 16. It was later decided that it was preferable for the MSC to be placed closer to the motor and inside the casing to reduce electrical losses from longer wiring, therefore this was built into the final design.

As it was necessary to reduce the overall weight of the scooter, the most desirable material to be used was Aluminium. A number of U-shaped channel pieces were considered for the fabrication of the battery casing, however most of these had very thick wall pieces that were not ideal. Use of these pieces would either add to the weight of the scooter or lead to wasted material in size reduction. Instead, after collaboration with the electrical and computer engineering (ECE) mechanical workshop technician, Mr. David Healy, it was decided that the piece could be fabricated from aluminium sheet metal. A final model was created by Mr. Healy, including provision for the MSC, and can be seen in Appendix 17. The design was realised with much success, fitting all components with room for wiring.

3.1.2 BLDC Hub Rim

The initial intention for the fitting of the BLDC rim was to find a similar sized wheel to fit the BLDC motor to the spokes of. When first purchased, the scooter had two 12" wheels however this size was found to be slightly too small for the BLDC to be fitted upon the spokes. The possibility of using larger wheels was explored however it was found that the discrete sizes manufactured meant that the next largest size would be 16" which was far too large. Therefore, to keep the scooter in proportion, the decision was made to fabricate a nylon rim for fitting of the BLDC hub. The model of this can be seen Appendix 18. This elegant solution worked very well, giving a very smooth ride and keeping the scooter wheels in proportion.

3.1.3 User Interface

Throttle

Due to the automotive nature of this project it was desirable to have a thumb throttle as opposed to a twist throttle in order to achieve a more stable means of control. Initially a mechanical thumb throttle was purchased for $14 NZD (inc. shipping). The intention was to fit this with a linear potentiometer to achieve an analogue value between 0-5V. Due to the physical nature of most potentiometers this proved to be too difficult and instead a linear Hall Effect thumb throttle was purchased from Golden Motors (see Figure 6) for a price of $42.96 NZD (inc. shipping).

The throttle gave a variable voltage from around 800mV – 3.5V which, while not ideal for resolution, could easily be scaled in software. Unfortunately, during the integration of the embedded system with the scooter, the throttle Hall Effect sensor was damaged and was no longer operational. This problem was resolved by replacing the part within the throttle with a Honeywell Hall Effect sensor purchased for $6.15 NZD [8] (inc. shipping). This worked to the advantage of the system as the new sensor achieved a linear voltage swing from 800mv through to 4.8V, a significant increase that would benefit the resolution.

Brake Button

The brake button was positioned on the left hand side of the handlebars (See Figure 6), incident to the mechanical braking lever. The button has been designed to transition from the on to off state when the level is pulled (see Appendix 11 for circuit). The appropriate signal can then be detected in software to deactivate the speed signal and activate the regenerative braking.

Boost Button

The boost button is placed on the right hand side of the handlebars at the full extension of the throttle (see Figure 6). The intention is that when the thumb throttle has been pushed to its limit, slightly more force can be applied to activate the boost overcurrent feature (see section 2.3 - i2t Overcurrent Algorithm). The idea being that the additional force required should be noticed by the user so they are aware that they have activated the boost overcurrent feature.

LCD Display and Embedded System Casing

The embedded system itself is encased on the centre of the handlebars (see Figure 7). Integrated into the case is an electrical isolation switch included as a safety precaution for development. The case also holds an LCD screen to relay information to the rider such as speed, remaining charge, which buttons are being pressed and whether boost is available (See Appendix 2 for user display manual).

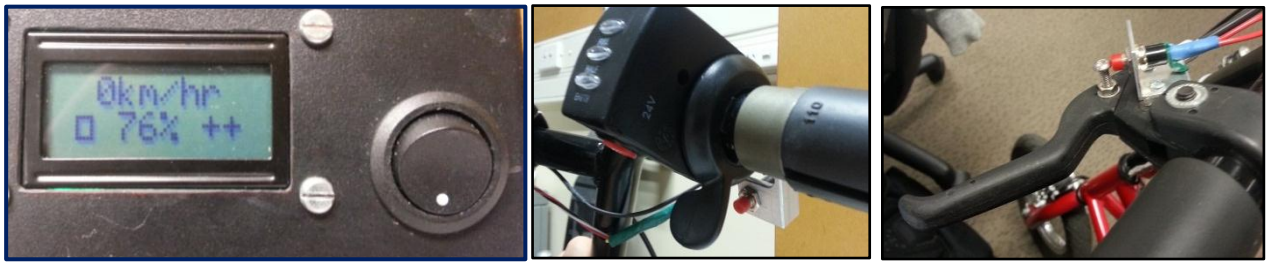

Figure 6 - LCD Display Interface (Left), Thumb Throttle and Boost Button (Centre) and the Brake Button (Right).

3.2 Embedded System

3.2.1 Hardware Design

To implement an effective control system for the scooter and relay the appropriate signals to the MSC, an embedded system was required. The core task of this system was to take the user inputs; throttle, brake and boost, apply control logic and then generate the desired speed and braking signals. Being an automotive application, a number of design elements had to be considered due to the noise generated from high motor currents.

Figure 7 - Photograph of Primary Board and its Housing Unit.

Microcontroller

The selected microcontroller unit (MCU) had to meet a certain selection criteria due to the devices it would be interfacing with and the peripherals required. The MSC operates with 5V logic so it was desirable for the MCU to use this same logic level so a translation chip would not be required. It was also a requirement for the MCU to have the following (See section 3.2.2 - System Inputs and 3.2.3 - System Outputs for peripheral applications):

- Two analogue to digital convertors (ADC), 10 bit precision or higher.
- At least 12 general purpose input/outputs (GPIO).
- A pulse width modulation (PWM) peripheral or digital to analogue convertor (DAC) output, 10 bit precision or higher.
- A timer peripheral.
- At least one external interrupt trigger.

The best suited MCU to this description, without an excessive pin, was the PIC18F25K50 from Microchip's PIC 18 series. The MCU cost $6.29 NZD and operates at a clock frequency of 8MHz. It has a 28 pin package and met all the requirements discussed above, with peripherals able to be multiplexed to variety of pins, allowing for flexible PCB layout [9].

PIKit3 Programmer

The selected MCU was able to be interfaced for programming using one of the departments PicKit3 USB to serial programmers. This simple in-circuit serial programmer (ISP) interface required only 3 pins (excluding supply pins) and allowed for debugging operation [10]. The MPLAB X integrated development environment (IDE) allowed for effective programming by utilising Microchip's extensive API library. The ISP configuration can be seen in Appendix 6.

PCB Manufacturer

The board was designed to utilise two layers and predominantly use surface mount devices (SMD). The initial intention was for the board to designed in the ECE department by Mr. Randy Hampton, the ECE Electronics Laboratory Technician, however as the complexity grew, as too did the number of vias in the design. As the department is unable to create plated through-hole vias, it was decided that it would be worthwhile for the final product to have the board manufactured externally. After discussions with Mr. Michael Cusdin, the department's Altium Design Consultant, it was arranged to have the board manufactured at Circuit Labs in Auckland for a price of $56 NZD (Four day turn-around).

Noise Considerations

As the board was to be placed upon the handlebars, with approximately a 1.2m separation from the MSC, the ribbon cable connecting the two devices would be vulnerable to conduct noise as an antenna. The effect of this is somewhat reduced owing to majority of the lead distance being encased within the metallic battery housing (See - 3.1.1 - Battery/Motor-Controller Housing). This would provide protection from noise to an extent by acting as surrounding Faraday Cage. To further avoid noise issues, filtering was required to different extents on each signal. Two different filters were implemented; a 2nd order low Pass Sallen-Key filter and a 1st order low pass RC filter each with cut-off frequencies discussed with respect to their application in subsequent sections.

Power Supply

The supply voltage to the board is nominally 26.4V, achieved from the 8 series sets of 3.3V cells. As the MCU requires a 5V supply, a voltage regulator was needed. The regulator selected was the LP38692MP-5.0 and cost $2.30. Power supply decoupling was added to ensure a stable supply voltage by adding two $100\mu F$ electrolytic capacitors from the regulated supply to ground (See Appendix 11). Additionally a 1A fuse was added for component protection should a short circuit occur. The system draws an average current of 24mA and 16mA in sleep mode, both very minimal when compared to the motor currents.

3.2.2 System Inputs

ADC Inputs – Current and Thumb Throttle Signal

The first ADC Input is the analogue voltage signal from the thumb throttle mounted on the handlebars. The 10-bit ADC allowed 1024 different voltage levels to be detected. In the context of this project having a supply of 5V the ADC was therefore capable of detecting changes in voltage given by,

$$\Delta V = \frac{V_{supply}}{2^{N_{bits}}} = \frac{5V}{2^{10}} = 4.9mV \quad (3)$$

where V_{supply} represents the 5V voltage supply and N represents the number of bits associated with the ADC. This is significantly better than the 19.5mV resolution that would be obtained by using an 8-bit ADC. The second ADC input is the current signal from the LEM Current Transducer (see section 3.3.1 - Current Transducer). As the voltage swing is not particularly large relative to

the supply voltage it was highly desirable to achieve a high voltage resolution meaning the 10 bit ADC was well utilised for this application.

GPIO and Interrupt Lines – Braking, Boost and Speed Signal

The remaining inputs to the board were digital signals and therefore able to be connected to GPIO pins. The first two of these were the brake and boost buttons. Due to the MCU clock speed being significantly higher than the rider's response to push either of these buttons it was sufficient for them to be polled upon timer interrupts as opposed to being connected to external interrupt lines (see section 3.4.1 - Standard Operation). Rather than dealing with the issue of button denouncing in software, additional circuitry was added to address the problem in hardware by slowing the response with a parallel capacitance (See Appendix 11 - Board Buttons).

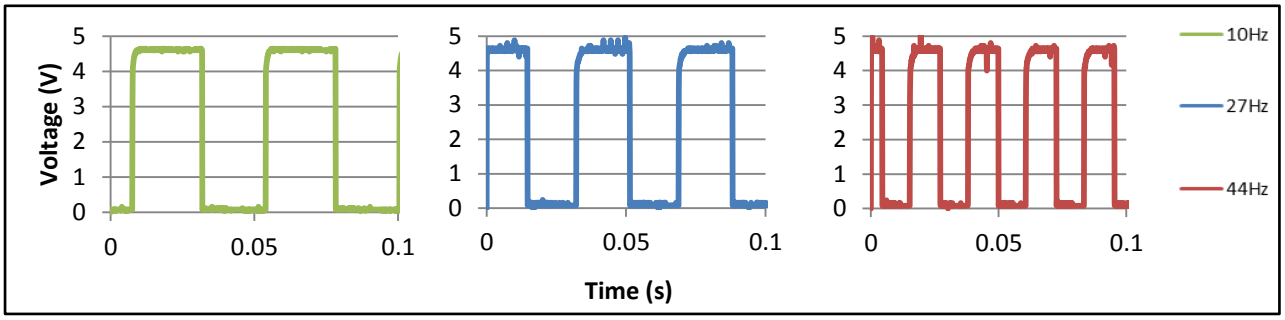

Figure 8 – BLDC Speed Signal at 5.6 km/hr (left), 15.3 km/hr (Centre) and 24 km/hr (Right).

The speed signal, shown above in Figure 8, is obtained from one of the Hall Effect sensors on the BLDC motor. It has been routed to one of external interrupt GPIO lines so that the period of the signal can be accurately measured by calculating the time difference between subsequent interrupts. The velocity of scooter can be calculated by equation 4 below, where N_{Hall} refers to the number of Hall Effect sensors, f_{signal} represents the signal frequency and scooter velocity, $V_{scooter}$, is measured in km /hr. As the frequency was not expected to exceed (45km/hr), a 1st order low pass RC filer with 80Hz cut off frequency was used to condition the signal from noise.

$$V_{scooter} = 3.6 \times 2\pi r \omega_{wheel} = \frac{7.2\,\pi\, r f_{signal}}{N_{Hall}} \quad (4)$$

3.2.3 System Outputs

PWM – Output Speed Signal

The PWM signal generated by the MCU operates at a frequency of 20 kHz. This value was used over higher frequencies as it allowed for a greater resolution of duty cycle (DC). This is owing to the DC of the signal being determined by the off time. The output PWM then goes through two stages of filtering. The first of these is a 1st order low-pass RC filter and is found on the primary board. The second stage of filtering happens on the secondary board, immediately before the MSC. This is a 2nd order low-pass Sallen-Key filter which also provides the signal with low output impedance. This provides appropriate energy transfer to the MSC. A cut-off frequency of 48Hz was

used for both filters as this was more than sufficient to smooth the 20 kHz signal but still allowed for fast changes in duty cycle (see Figure 9 for filtered signal on the following page).

GPIO – Regenerative Braking

The regenerative braking output signal is run from one of the MCU's GPIO through the secondary board to the MSC. The MSC regenerate braking pin is high by default and needed to be pulled low to activate the braking. Upon implementation it was found that the MCU was unable to sink enough current to do this directly and pull down resistor of $1k\Omega$ was added. This change was made on the secondary board and allowed regenerative braking to function effectively.

3.2.4 LCD Interfacing

The MIDAS - MC20805A6W LCD 2x8 character alphanumeric screen (see Figure 6) was able to be interfaced with the MCU by using seven GPIO pins, of which, four are data pins and three are control pins. This was possible due to LCD module's HD44780 controller which supported a four bit addressing mode. This came at a small cost of longer read/write duration, however, due to the high speed of the MCU clock and the limitations of the human eye this was not an issue. The LCD display cost $ 17.93.

3.3 Secondary Board

In order to maintain signal integrity, a secondary board (See Figure 9) was designed to mount the current transducer close to the BLDC motor and MSC (See Appendix 3 for board location). The circuit was of relatively low complexity compared to the primary board. For this reason it was able to be fabricated in the ECE department. The schematic and PCB layout for this board can be seen in Appendix 13 and Appendix 14 respectively.

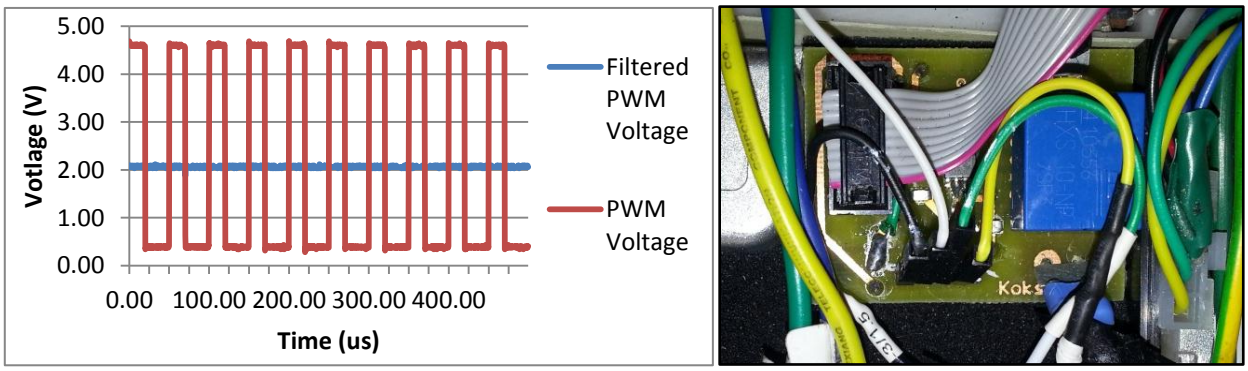

Figure 9 - PWM Filtering at 40% Duty Cycle (Left) and Secondary Board (Right).

3.3.1 Current Transducer

The main component of the board, the current transducer, is a LEM HXS 10-NP/SP3 Hall Effect sensor connected in series with the current supply to the BLDC motor. The component cost $21.50. The signal output from the sensor is relayed back through a ribbon cable to the embedded system board on the handlebars to be used in over current monitoring and control implementation. The current transducer is connected in a series configuration giving a voltage swing of 2.5V to 5V corresponding to a 0A to 30A current range. This signal is then passed through

a 2nd order low pass Sallen-Key filter on the primary board before being sampled by an ADC. The cut-off of this filter is 48Hz to attenuate any high frequency noise generated by high current while leaving an average current signal to be sampled.

3.3.2 PWM Filtering

The 2nd stage of PWM filtering is implemented through another 2nd order low pass Sallen-Key filter on the secondary board so that the signal is conditioned immediately before the MSC and provides a low impedance output (See PWM in section 3.2.3 -System Outputs).

3.4 Software Design and Control Strategy

In order for the software to be developed while mechanical modifications were being carried out and the circuit boards were being printed, a developer's board was purchased. This worked well for the development and abstraction of hardware independent peripherals such as the ADC, PWM, timer and interrupt routines. These abstractions were all able to be incorporated in the final software design. The following sections discus the real time operating system running on the direct drive electric scooter and the tasks that are being executed.

3.4.1 Standard Operation

The real time operating system running the scooter is built up of two sets of tasks; those running in the back ground that are not time critical and those running in the foreground that are either event driven or time critical. The tasks from both sections are described below.

Foreground Tasks

With the exception of the speed signal interrupt, all foreground tasks run off a half millisecond timer interrupt. Each time the interrupt occurs the following tasks are carried out in the following order.

1) The real time clock is updated (Used for determining period of speed signal).
2) A state machine alternates between sampling the current ADC and throttle ADC (i.e. each are sampled at $2\ interupts \times \frac{1}{2} ms\ per\ interupt = 1ms$).
3) Brake and boost GPIO lines are read.
4) Current control calculations are carried out. (see 3.4.2 - Over Current Prevention).
5) Motor speed PWM and regenerative braking signals are set based on values obtained from tasks (2), (3) and (4).

Background Tasks

The first of the remaining background tasks is the LCD display update routine as it is not time critical and is of lower priority than the tasks described above. The second background task a timeout check is carried out and puts the system to sleep if motion has not been detected for ten seconds. This is both to save power and so that the system never has to be manually switched off. As a result, the system can retain memory of remaining battery charge. As the speed signal generated by the Hall Effect sensors is connected to one of the MCU interrupt lines, the system will automatically become active once again once motion is returned.

Battery Charge Monitoring

The amount of charge that has been drawn from cells is calculated by integrating the current signal sampled by the MCU. This can then be subtracted from the total battery charge and displayed as percentage. In order for this information to be retained in random access memory (RAM) the MCU cannot be reset and instead the previously described sleep mode is used.

3.4.2 Over Current Prevention

In standard operation, when the boost button has not been pressed, the software needs to manually limit the current supplied to the motor to below what it is rated for. This was difficult to implement as a control system for two reasons. First because the rated current was a limit and not a target therefore error could only be accumulated in one direction. The second reason was that the actuator value, desired speed, was not necessarily proportional to current and instead was function of the mechanical load being exerted on the BLDC motor. Figure 10 below shows a block diagram illustrating the control procedure in place on the scooter.

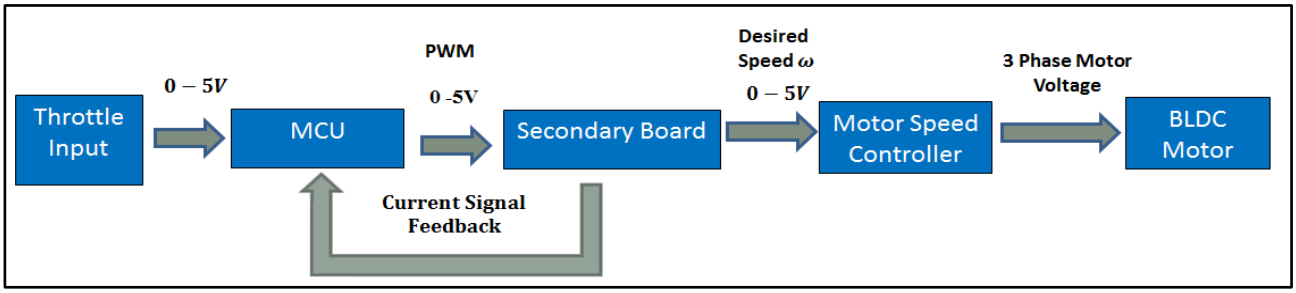

Figure 10 - Block Diagram illustrating the Standard Control Structure.

A proportional integral (PI) controller was created to limit current to the rated value when the boost button had not been pressed. The integral portion of the control structure only ever acts to reduce the output desired speed value and thus attempt to reduce the current. The resultant PI controller can be seen to work below in Figure 11 where nominally the current is limited to 300mA (no load test condition) and then extended to 600mA during a boost period of 15 seconds. The negative spikes shows short pules of regenerative braking.

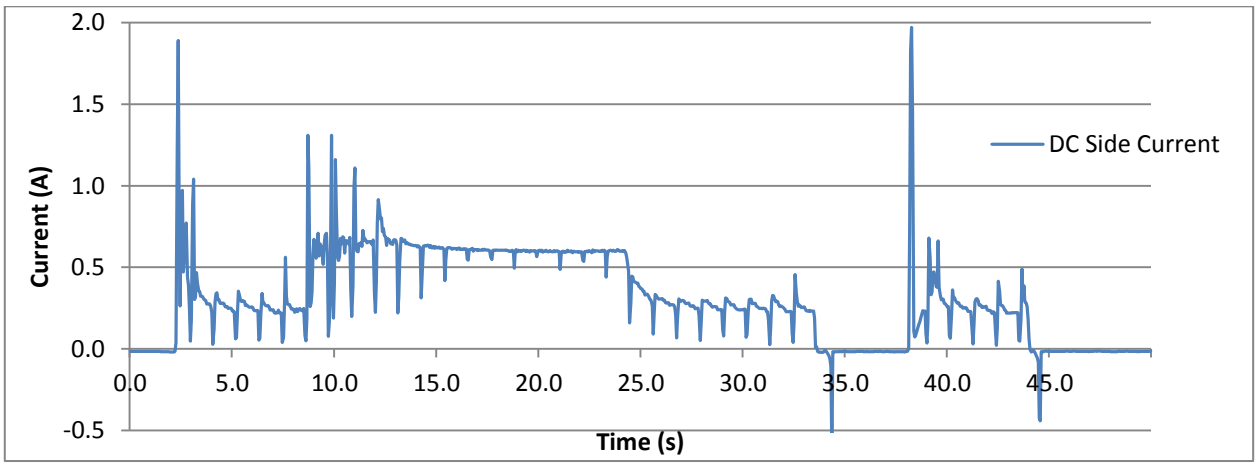

Figure 11 - DC Side Current Waveform (No Mechanical Load)

3.4.3 i^2t Overcurrent Algorithm

The i^2t overcurrent algorithm is constantly running as part of task 4 in the foreground tasks (See 3.4.1 Standard Operation). Figure 12 below shows a block diagram illustrating the process involved. Each time the current signal is sampled, the difference between the squared values of measured and rated current is added to the i^2t tracking variable. In standard operation this value would remain zero however when the boost button is pressed at the full extension of the throttle, the PI controller previously described is extended to limit the current to twice the rated current. As the measured current is now greater than the rated current the tracking variable begins to increase. If this value exceeds the i^2t limit calculated by equation 1 the boost feature is disengaged and notified on the display. The current is then limited back to I_{rated} until the i^2t product drops to below half of the i^2t limit before being made available once again. The result of this system can be seen on the previous page in Figure 11 as the no load current is extended to twice the hypothetical rated current for 15 seconds.

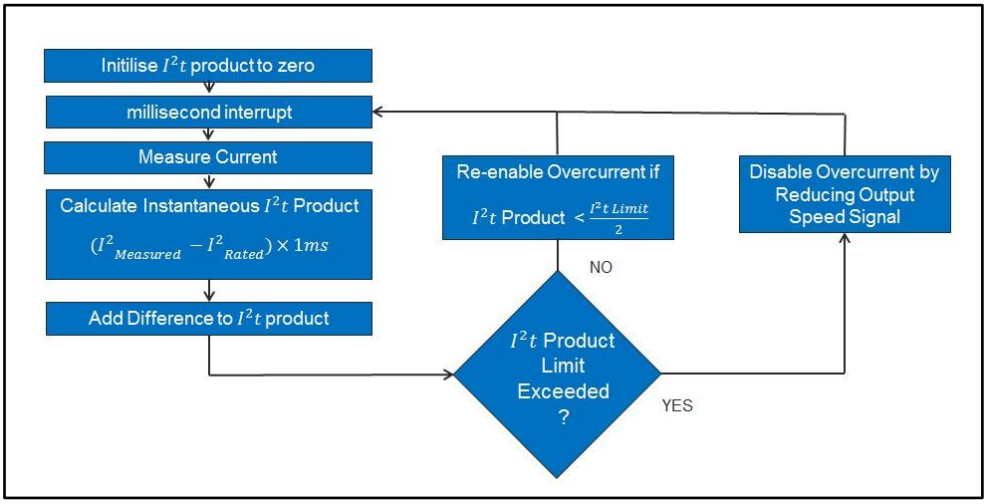

Figure 12 - Flow Diagram Illustrating the i^2t Algorithm.

3.4.4 Additional Functionality – Rolling Start

During development it was discovered that the BLDC motor/MSC combination as unable to accelerate from standstill. This is due to rotor position initially being unknown. As a result, the MSC attempts to apply a force to a phase in order to gain a reading from a Hall Effect sensor. This method fails when the motor is under mechanical load and therefore a rolling start requirement was implemented on the MCU. That is, that the scooter will not send a speed signal to the MSC unless the scooter is traveling greater than 2km/hr. This has little effect on the rider as scooter is typically pushed off. The effect of this is also an extended battery life as the most current is drawn at the initial acceleration. Furthermore it provides a safety measure that the scooter cannot be accelerated if the throttle is accidentally triggered when stationary.

3.5 Motor Waveforms

To assess the performance of the direct drive electric scooter two key waveforms must be examined. Figure 13 on the following page shows the DC side current waveform as the system is

limited to a specified rated current of 4A under a mechanical load. At t= 8 seconds, the boost feature is engaged to allow the current to exceed this rated current (up to 8A). The system is pre-specified to be able to run at twice this rated current for up to three seconds. As the mechanical load is not great enough to cause the motor speed controller to draw such a current, the system instead draws approximately 4.8A for a shorter duration. This duration will correspond to the i^2t limit set by these parameters. By observing Figure 13 it can be seen that this is approximately eight seconds at 4.8A.

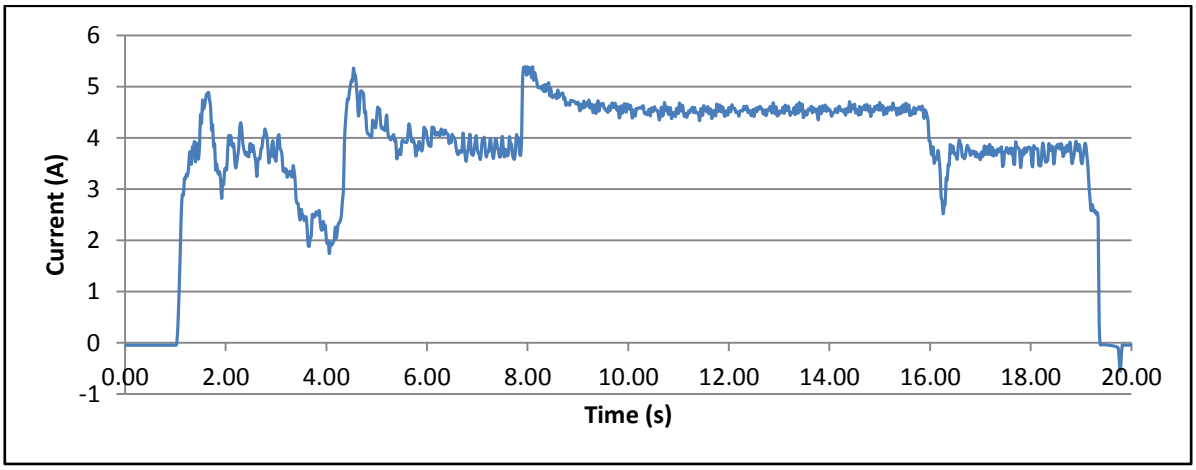

Figure 13 – DC Side Current Waveforms (Under Mechanical load).

It is also important to observe the three phase trapezoidal voltage signals generated by the MSC and applied to the BLDC motor. Figure 14 below shows the three phase to ground voltage signals, their moving averages and the DC side current being drawn. The voltage signals shown are very noisy due to the back EMF being produce by the motor. The moving average signals agree with the theory discussed in section 2.1 - Brushless Direct Current Hub Motor, by resembling the trapezoidal voltage waveforms separated by a phase of 120 degrees from one another. This confirms the BLDC motor and the MSC outputs are operating correctly.

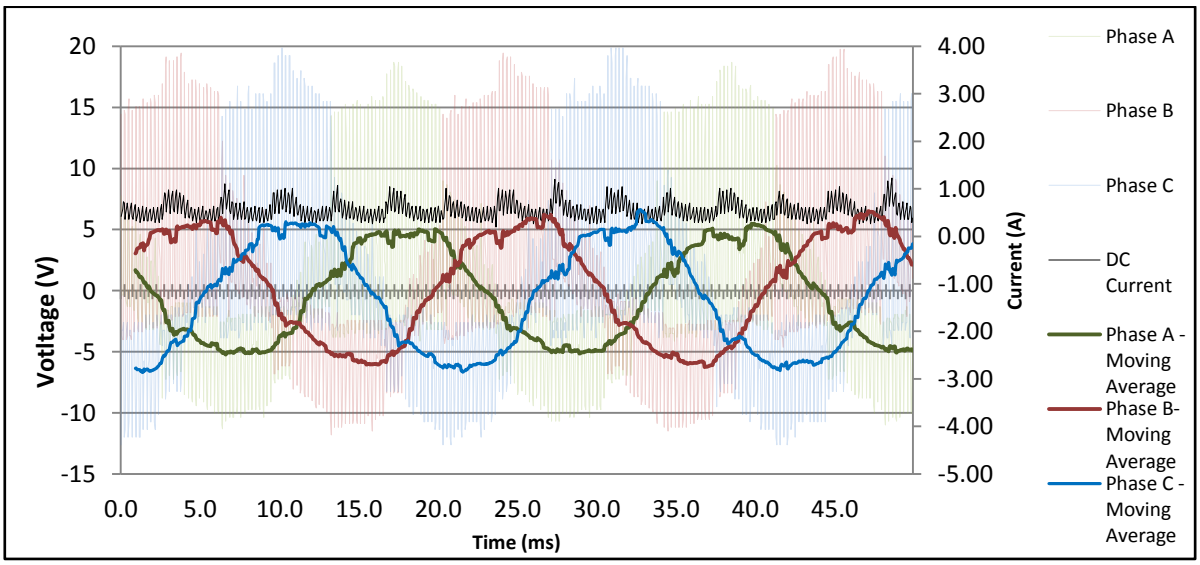

Figure 14 – BLDC Phase to Ground Voltage Waveforms and DC Side Current Supply.

4. CONCLUSION

The direct drive electric scooter project can be considered to be a success as it meets all of the criteria specified prior to project commencement. The scooter is capable of, speeds of 15 km/hr on flat surfaces although it does struggle with inclines. Regenerative braking has been successfully implemented, however has only been shown in short bursts of negative current due to the difficulties of measurements on a moving scooter. It does however function as an effective means of electrical braking. The expected range, given the cell energy capacity of 303.6 Whr, is 20km. This satisfies the original motivation of providing an alternative form of short range transportation for urban areas. Both the range and speed are adequate to substitute the direct drive eclectic scooter for many other short range light vehicles.

The 'boost' feature utilising the over current algorithm has been successfully implemented. Unfortunately the algorithm has only been able to be tested for light mechanical loads, and therefore scaled down current limits, due to the inability of the mechanical load to cause enough current to be drawn (See Appendix 8). It is expected, however, that the system at these low loads should have no issue when scaled up to full loads. In terms of the control implementation, the only difference is a greater feedback current value from the current sensor.

The methodology of splitting the project into three parallel streams of development worked very well to utilize time most effectively and ensure that there were few periods where work was unable to be carried out on the project. In particular the developer's board proved to be a very beneficial development platform by eliminating any possibility of hardware issues.

The design and development of the direct drive electric scooter was not without problems. During the final stages of development, two of the eight sets of five-paralleled cells were discharged to a damaging point (ten damaged in total). The supply was able to be restored by removing one of the side sets of cells (now containing six functional cells) and, combining with two spare cells to replace the damaged area (see Appendix 3 for concerned areas).

The project would be most benefitted by future improvements to two main areas. The first of these would be the formation of a more defined control structure that more effectively deals with the control of current through means of adjusting the desired velocity to the MSC. This could alternatively be dealt with by using a MSC with current control however there is most likely a control method that could accommodate for this indirect control appropriately. The second potential area of improvement concerns BLDC motor itself, namely investigation into alternative motors that could utilise the high current discharge properties of the LPF cells. This would benefit the scooters ability to deal with inclines; however it would reduce the expected range.

5. REFERENCES

[1] M. Codlin, “Making An Electrical Bicycle Better: Battery and Motor Controller Upgrade,” University of Canterbury, Christchurch, 2012.

[2] Texas Instruments, “Trapezoidal Control of BLDC Motors,” February 2010. [Online]. Available: https://www.google.co.nz/url?sa=t&rct=j&q=&esrc=s&source=web&cd=1&ved=0CC0QFjAA&url=http%3A%2F%2Fe2e.ti.com%2Fcfs-file.ashx%2F__key%2Ftelligent-evolution-components-attachments%2F00-171-01-00-00-14-23-21%2FTrapezoidal-Control-of-BLDC-Motors-Using-Hall-Eff. [Accessed 22 August 2013].

[3] P. Yedamale, “Brushless DC (BLDC) motor fundamentals,” 2003. [Online]. Available: http://electrathonoftampabay.org/www/Documents/Motors/Brushless%20DC%20(BLDC)%20Motor%20Fundamentals.pdf. [Accessed 21 August 2013].

[4] Golden Motors, “Cruise Controller User Guide,” 6 October 2009. [Online]. Available: http://www.goldenmotor.com/. [Accessed 14 July 2013].

[5] Copley Controls Corp, “Protecting Motors against overload conditions,” 6 June 2001. [Online]. Available: http://www.copleycontrols.com/motion/pdf/IsqT.pdf. [Accessed 6 July 2013].

[6] A123Systems, *Proper Assembly of A123Systems High Power Lithium-ion Cells into High Voltage and High Capacity Strings,* Watertown: A123Systems.

[7] Massachusetts Institute of Technology, “The BWD Scooter,” 11 July 2009. [Online]. Available: http://web.mit.edu/first/scooter/. [Accessed 14 September 2013].

[8] Honeywell, “SS490 Series Standard Miniature Ratiometric Linear Sensors, Radial,” [Online]. Available: http://docs-asia.electrocomponents.com/webdocs/009a/0900766b8009a37c.pdf. [Accessed 8 August 2013].

[9] Microchip, “28/40/44-Pin, Low-Power, High-Performance Microcontrollers with XLP Technology,” 29 November 2011. [Online]. Available: http://ww1.microchip.com/downloads/en/DeviceDoc/30684A.pdf. [Accessed 6 July 2013].

[10] Microchip, “PICkit 3 In-Circuit Debugger,” [Online]. Available: http://www.microchip.com/stellent/idcplg?IdcService=SS_GET_PAGE&nodeId=1406&dDocName=en538340&redirects=pickit3. [Accessed 6 July 2013].

6. APPENDICES

Appendix 1 – Side View of Direct Drive Electric Scooter Illustrating System Locations.

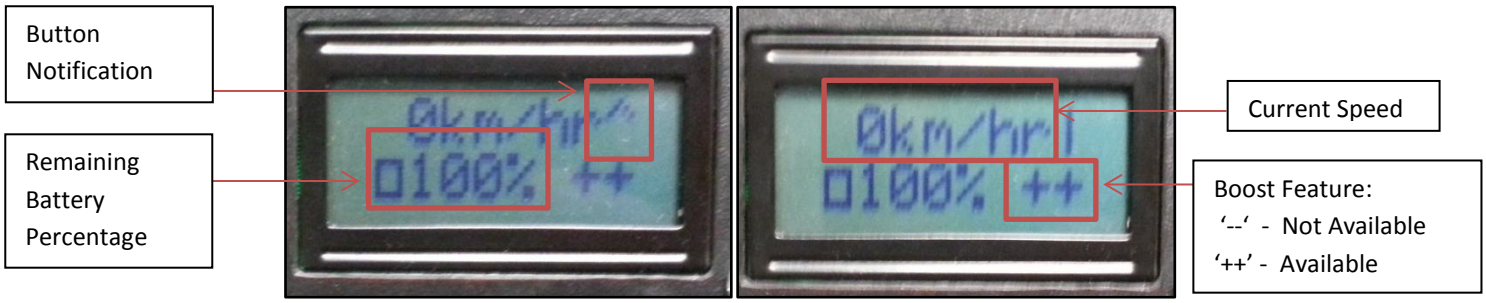

Appendix 2 – User Interface While Boost button is Pressed (Left) and While Brake is Pressed (Right).

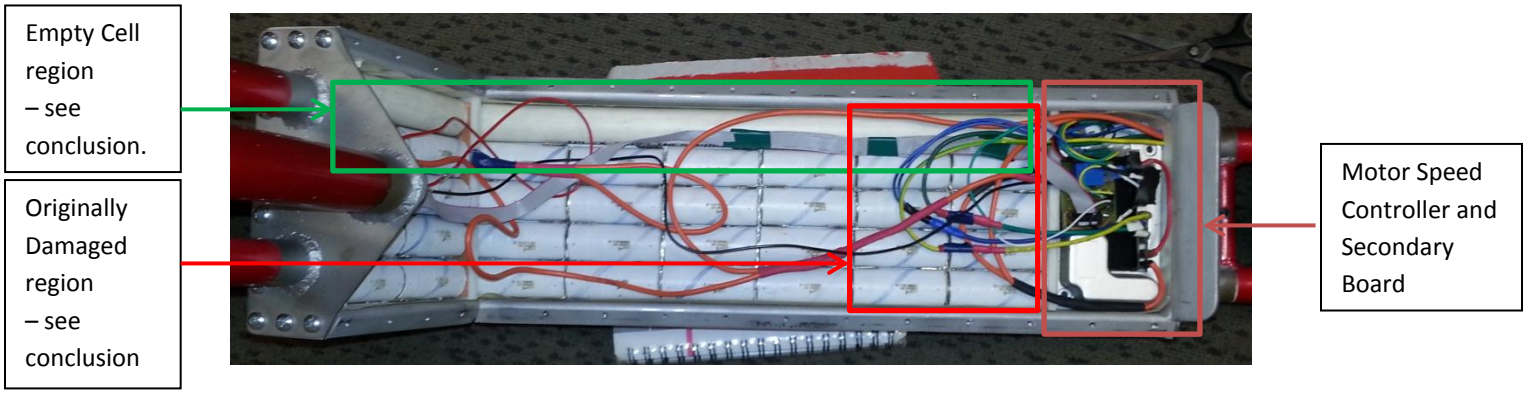

Appendix 3 – Top View of Battery Housing of the Direct Drive Electric Scooter Illustrating Secondary Boards Location.

Appendix 4 - Costs of purchases already made by the department.

Item Name:	**Cost:**
40 x A123 $LiFePO_2$ Cells	$ 170.20
Motor Speed Controller	$ 75
BLDC Hub Motor	$ 220
Scooter	$ 50
Total:	$ 512.20

Appendix 5 - Costs of Purchases Made for the Final Direct Drive Electric Scooter Design (Exc. Workshop Parts and Labour).

Item Name:	**Cost:**
Microcontroller - PIC18F25K50	$ 6.29
Circuit Labs - PCB Fabrication	$ 56
LEM - Current Transducer	$ 21.50
Other Electrical Components (Resistors, Capacitors, Diodes and Fuses)	$ 9.80
Operational Amplifier x 2 - AD548JRZ	$ 12.30
Voltage Regulator	$ 2.30
Golden Motor Thumb Throttle	$ 42.96
Throttle Replacement Hall Effect Sensor	$ 6.15
Handlebars	$ 35
LCD Display	$ 17.93
Total:	$ 210.23

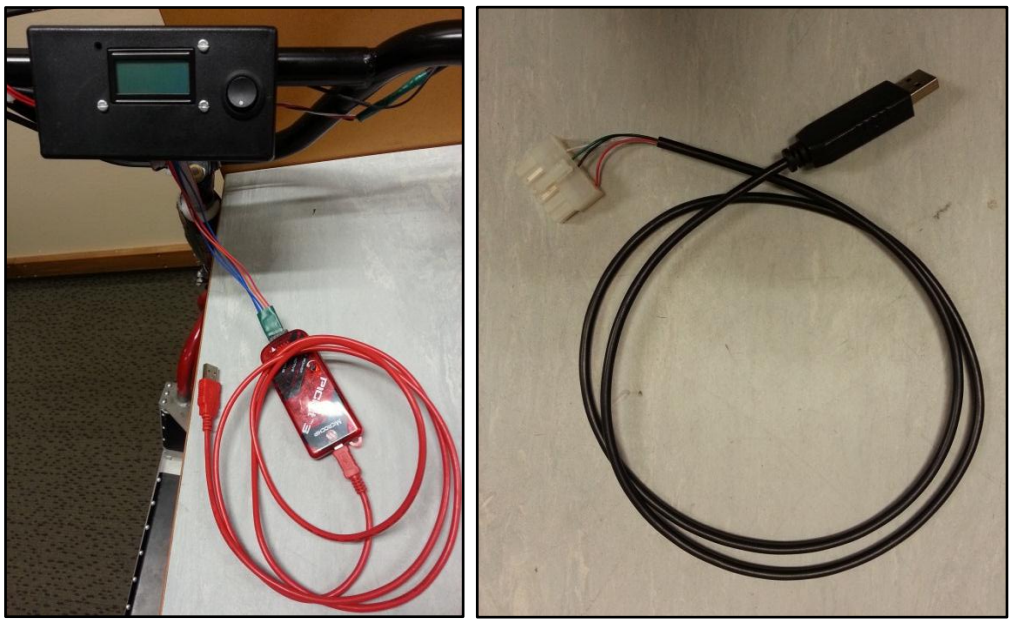

Appendix 6 - ISP Programmer for the MCU (Left) and the proprietary cable for configuring the golden motor MSC.

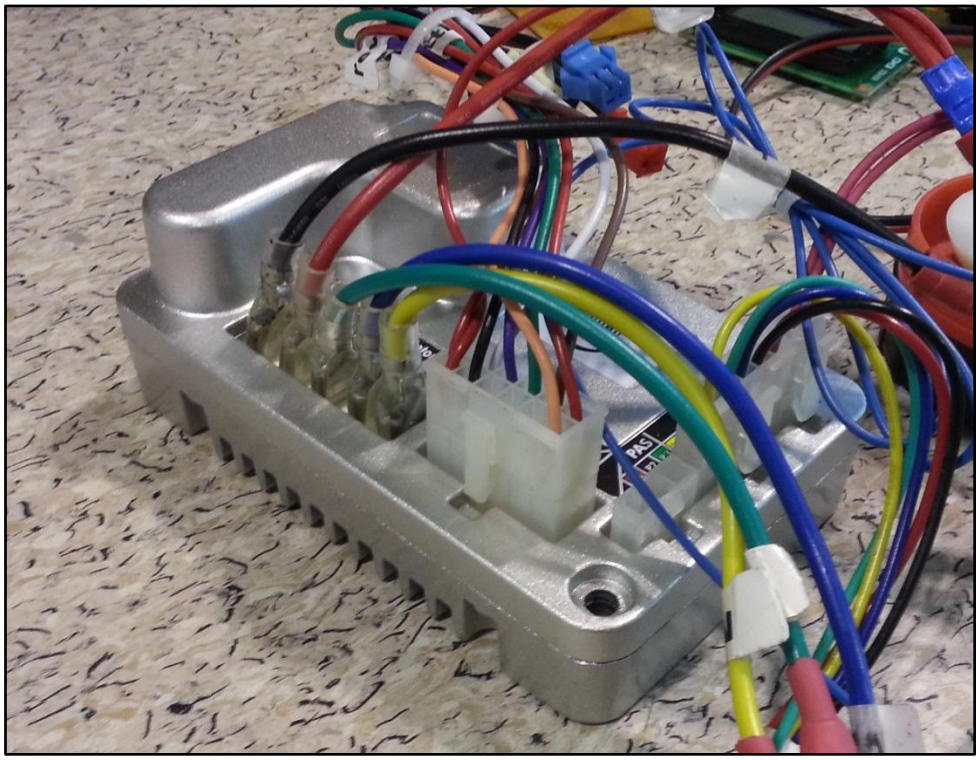

Appendix 7 – Golden Motor BAC-0281 Motor Speed Controller.

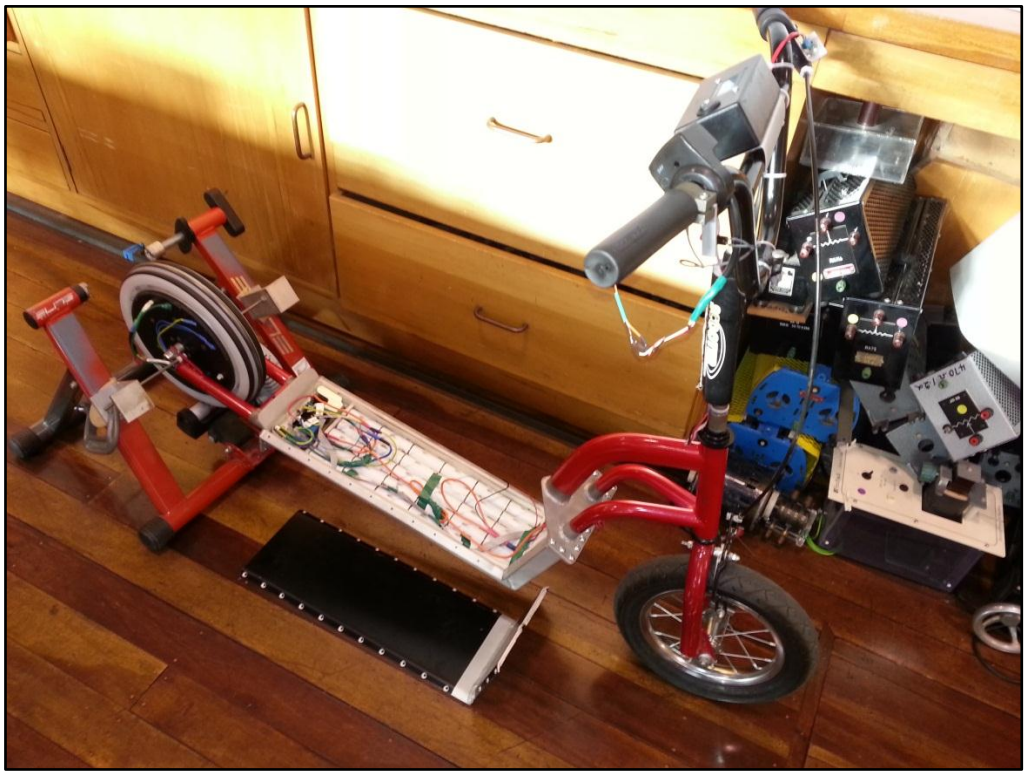

Appendix 8 – Direct Drive Electric Scooter Attached to Mechanical Test Rig.

Bill of Materials

Bill of Materials For Project [Scooter - Primary Board - Project .PrjPCB] (No PC

Source Data From: Scooter - Primary Board - Project .PrjPCB
Project: Scooter - Primary Board - Project .PrjPCB
Variant: None

Creation Date: 9/16/2013 4:42:29 AM
Print Date: 41533 41533.19621

Footprint	Comment	LibRef	Designator	Description	Quantity
RESC1608L	20k	RS_10K	20l, R4	RES 10.0K OHM 1/10W 5% 0603 SMD	2
CAPC1608L	1uF	CC_1uF_0603	C1, C2	CAP CER 1uF Y5V -20% +80% 16V 0603	2
CAPC1608L	100nF	CC_100nF_0603, CC_100nF_0603, CC_100nF_0603, CC_100nF_0603, CC_100nF_0603, CC_100nF_0603, CC_220nF_0603, CC_100nF_0603	C3, C4, C5, C8, C9, C10, C11, C19	CAP CER 100nF X7R +-10% 50V 0603, CAP CER 100nF X7R +-10% 50V 0603, CAP CER 100nF X7R +-10% 50V 0603, CAP CER 100nF X7R +-10% 50V 0603, CAP CER 100nF X7R +-10% 50V 0603, CAP CER 100nF X7R +-10% 50V 0603, CAP CER 220nF Y5V -20% +80% 16V 0603, CAP CER 100nF	8
CAPC1608L	10nF	CC_10nF_0603	C7, C13, C14	CAP CER 10nF X7R +-10% 50V 0603	3
NICH-1	100uF/16V	CA_100uF_16V_SMD	C17, C18	Nichcon WX series SMT Aluminium Electrolytic Cap	2
LED0.8X1.6	#NAME?	DL_TLMG1100	D1	LED Green 0603	1
RESC3216N	1A	FS_Fuse_1.0A_SMD_1206	F1	Fuse 1.0A Very Fast Acting 1206	1
HDR2X8	Header 8X2	Header 8X2	H1	Header, 8-Pin, Dual row	1
HDR1X5	Header 5	Header 5	H3	Header, 5-Pin	1
IDC2.54-V10D	Header 5X2 Vert	JA_HDR_IDC_5X2_VERT	H4, H5	IDC Header, 2,54mm, 10-Pin, Vert	2
MOLEX_KK_2_HDR	2 Pin Molex KK HDR	JA_MOLEX_KK_2POS	H6	CONN HEADER 2POS 2.54mm VERT_Thru Hole	1
RESC1608L	10K	RS_10K, RS_10K, RS_10K, RS_470R, RS_10K, RS_10K	R1, R2, R9, R19, R22, R23	RES 10.0K OHM 1/10W 5% 0603 SMD, RES 10.0K OHM 1/10W 5% 0603 SMD, RES 10.0K OHM 1/10W 5% 0603 SMD, RES 470 OHM 1/10W 5% 0603 SMD, RES 10.0K OHM 1/10W 5% 0603 SMD, RES 10.0K OHM 1/10W 5% 0603 SMD	6
RESC1608L	147	RS_10K	R3	RES 10.0K OHM 1/10W 5% 0603 SMD	1
RESC1608L	33k	RS_10K	R5, R6, R21	RES 10.0K OHM 1/10W 5% 0603 SMD	3
RESC1608L	470R	RS_470R	R10, R20, R24	RES 470 OHM 1/10W 5% 0603 SMD	3
RESC1608L	100R	RS_470R	R15	RES 470 OHM 1/10W 5% 0603 SMD	1
EVQPNF05M	EVQPNF05M	WS_EVQPNF05M	S2	Panasonic 6 x 3.5mm SMD Light Touch Switch Type	1
SOT223-5N	LP38692	MCP1826-ADJE/AT	U1	1000 mA, Low Voltage, Low Quiescent Current LDO Regulator, 5-Pin TO-220, Extended Temperature	1
SO8_N	uA741C	LM101AJG	U2	High Performance Operational Amplifier	1
SOIC-SO28_N	PIC18F25K50-I/SO	PIC18F25K20T-I/SO	U3	Flash Microcontroller with 10-Bit A/D and nanoWatt Technology, 32K Flash, 28-Pin SOIC, Industrial Temperature Range, Tape and Reel	1
					42

Approved	Notes	

Appendix 9 – Primary Board Bill of Materials.

Bill of Materials

Source Data From: Scooter - Secondary Board - Project.PrjPCB
Project: Scooter - Secondary Board - Project.PrjPCB
Variant: None

Creation Date: 9/16/2013 4:43:05 AM
Print Date: 41533 41533.19662

Footprint	Comment	LibRef	Designator	Description	Quantity
CAPC1608L	100nF	CC_100nF_0603	C4, C5	CAP CER 100nF X7R +-10% 50V 0603	2
MOLEX_KK_2_HDR	2 Pin Molex KK HDR	JA_MOLEX_KK_2POS	H1, H2	CONN HEADER 2POS 2.54mm VERT_Thru Hole	2
HDR1X7	Header	Header 7	P1	Header, 7-Pin	1
HDR1X5	Header 5	Header 5	P2	Header, 5-Pin	1
RESC1608L	33k	RS_10K	R5, R6	RES 10.0K OHM 1/10W 5% 0603 SMD	2
SO8_N	uA741C	LM101AJG	U2	High Performance Operational Amplifier	1
PCBComponent_1	LEM - HXS 10-NP/SP3	TC1072-3.0VCH713	U4	50mA and 100mA CMOS LDOs with Shutdown, Active-Low Error Output and VREF Bypass, 6-Pin SOT-23, Extended Temperature, Tape and Reel	1
					10

Approved **Notes**

Appendix 10 – Secondary Board Bill of Materials.

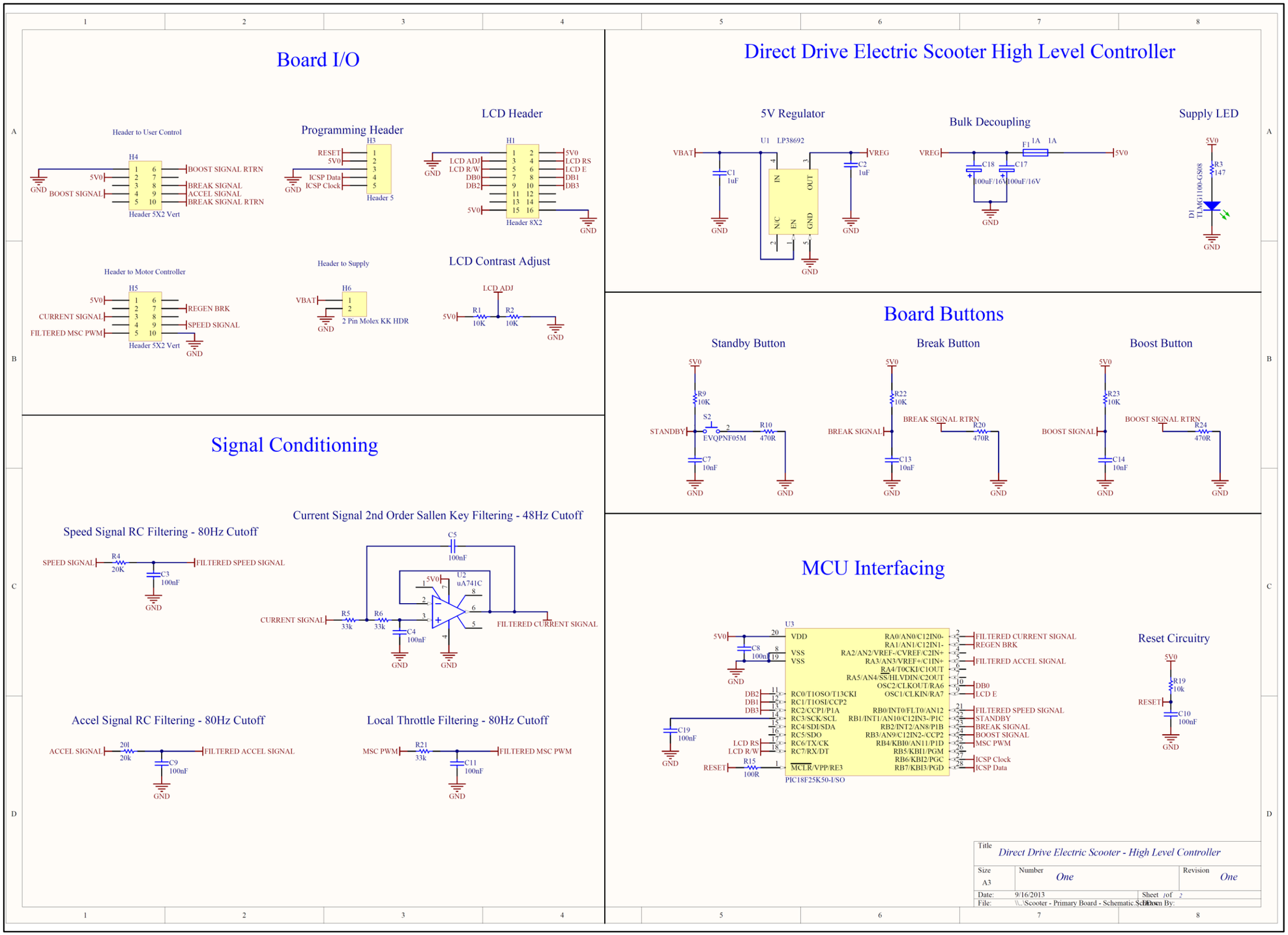

Appendix 11 - Primary Board Schematic.

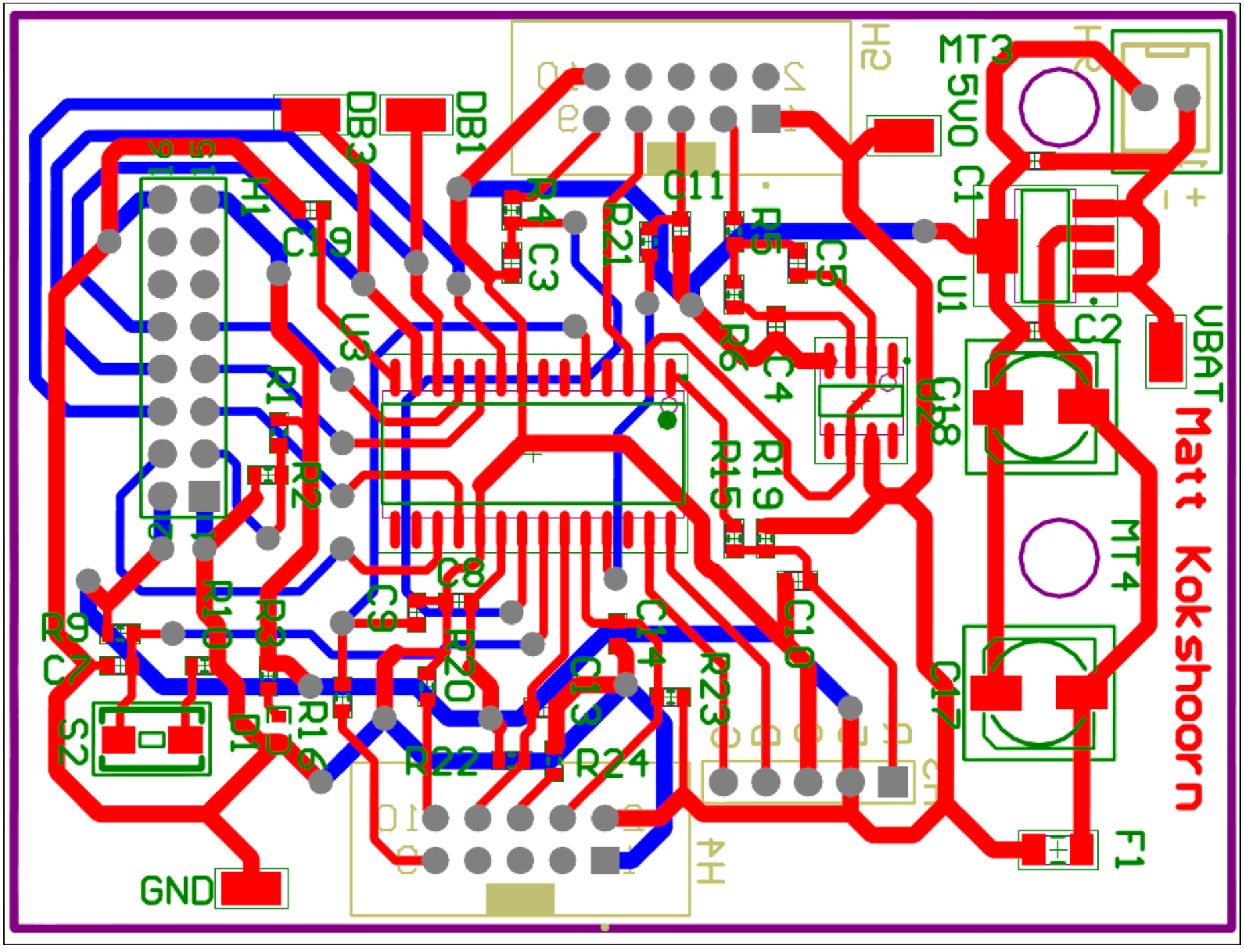

Appendix 12 - Primary Board PCB Artwork.

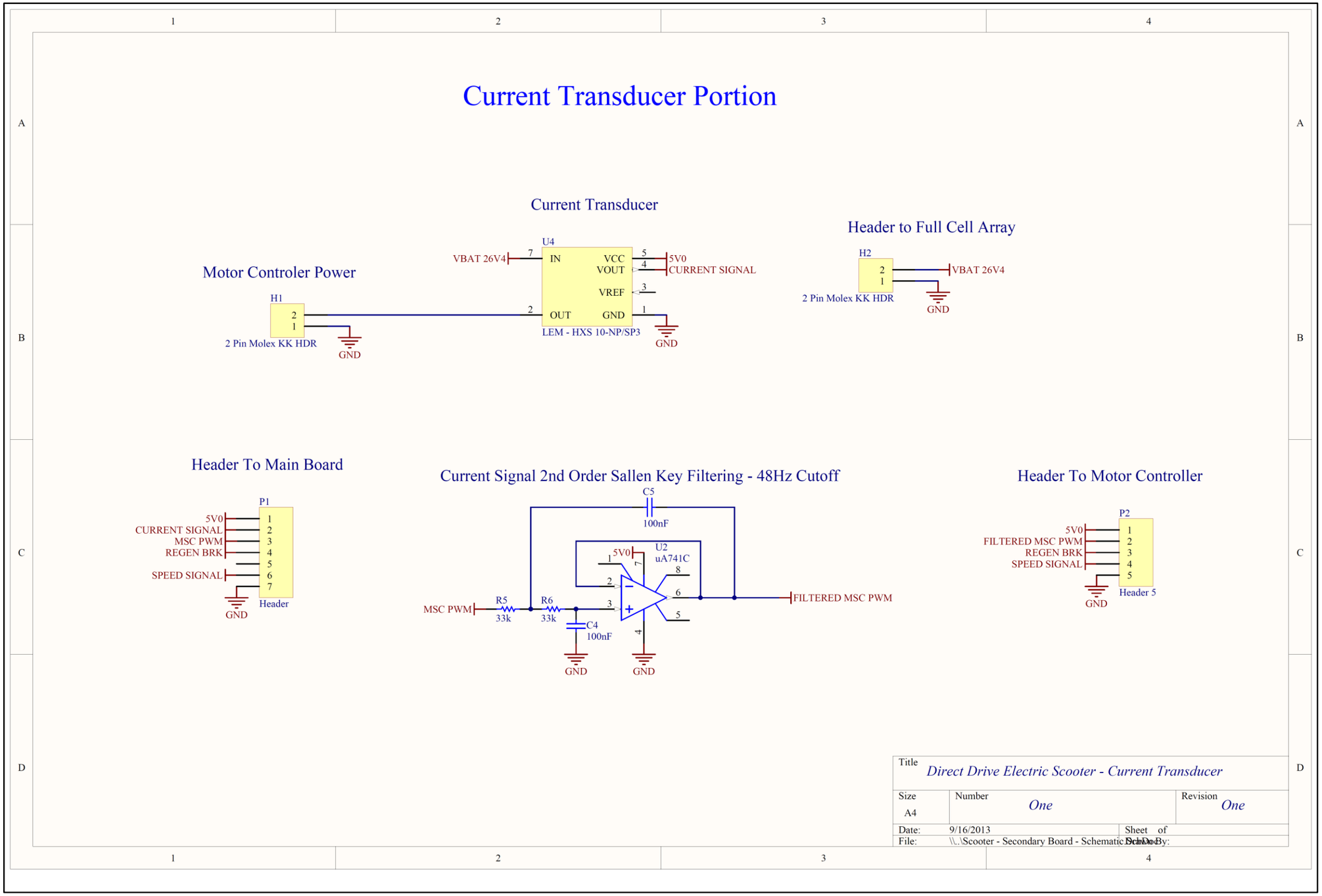

Appendix 13 – Secondary Board Schematic.

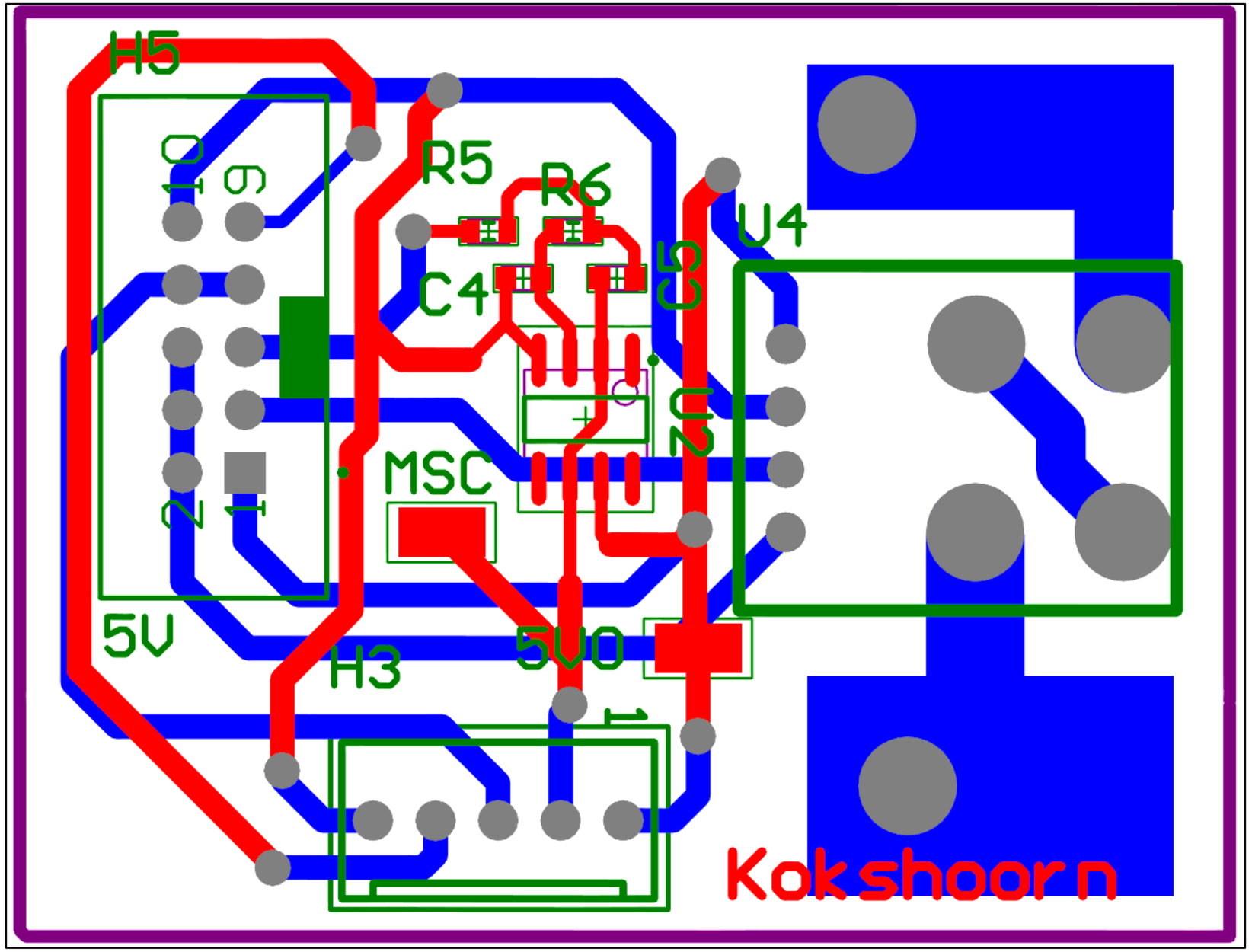

Appendix 14 - Secondary Board PCB Artwork.

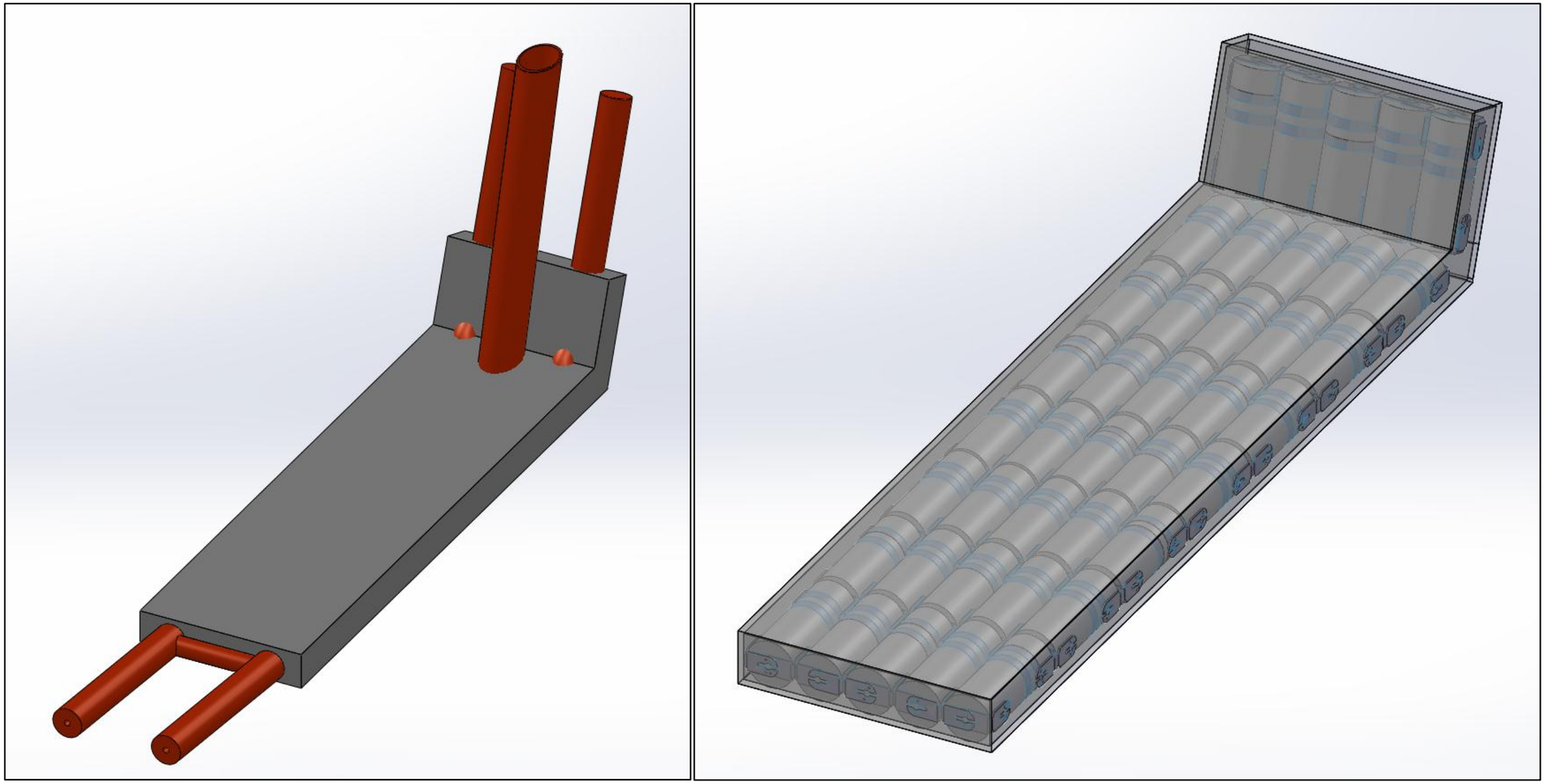

Appendix 15 - Initial Battery Housing Solid Works Model With Frame (Left) and Transparent Without Frame (Right).

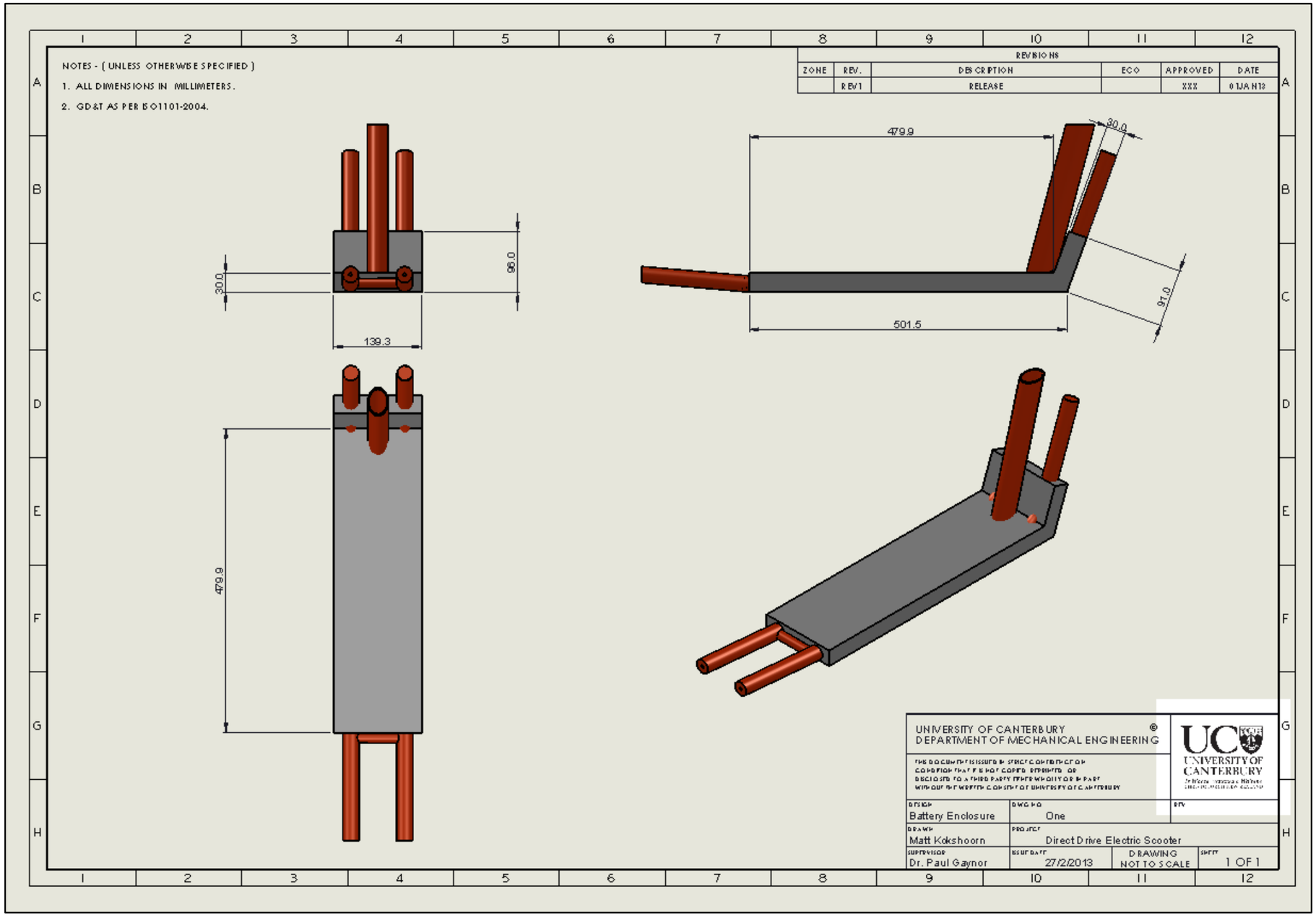

Appendix 16 - Initial Battery Housing Solid Works Drawing.

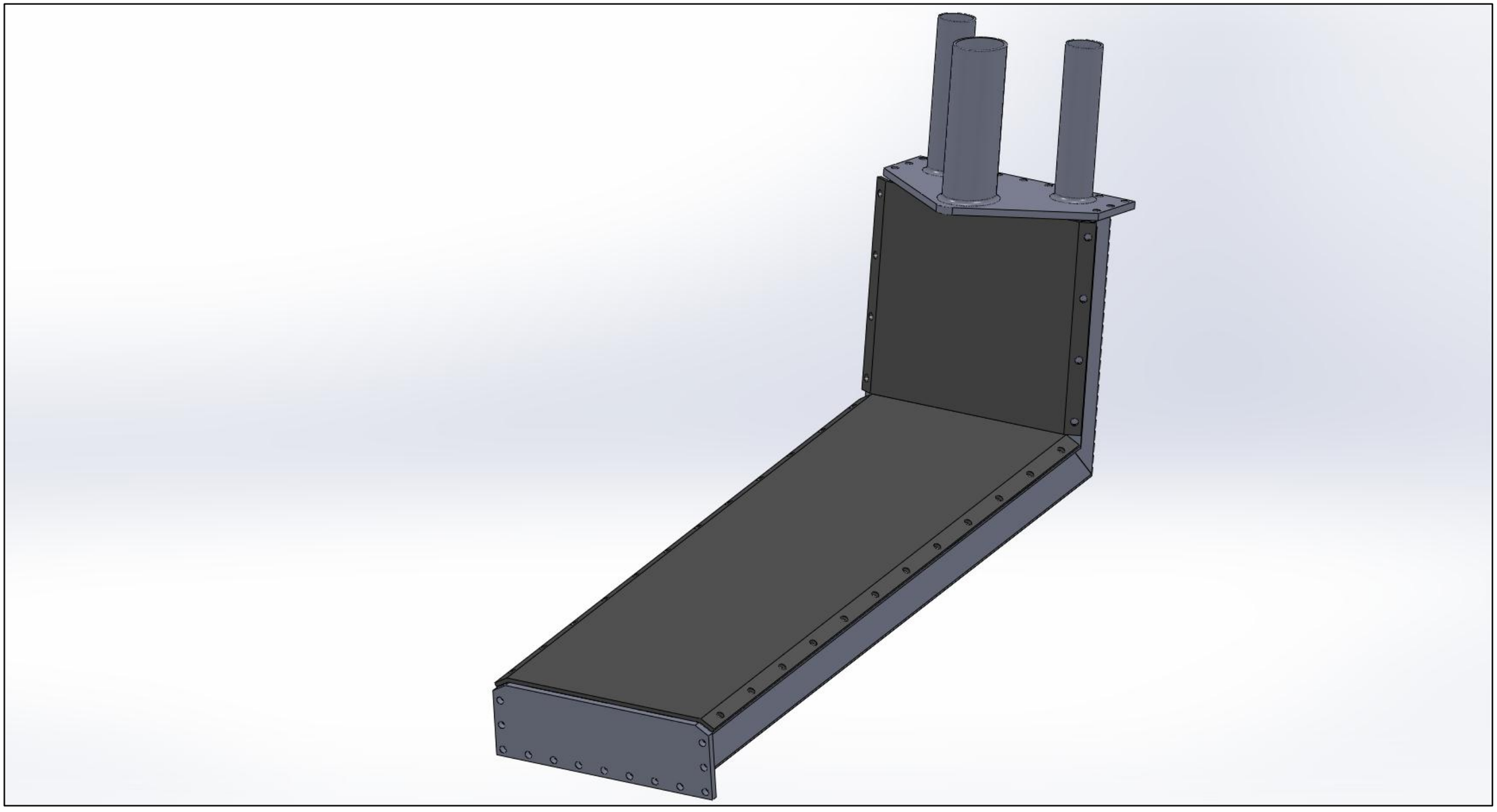

Appendix 17 – Final Battery Housing Solid Works Model – (Modelled By David Healy).

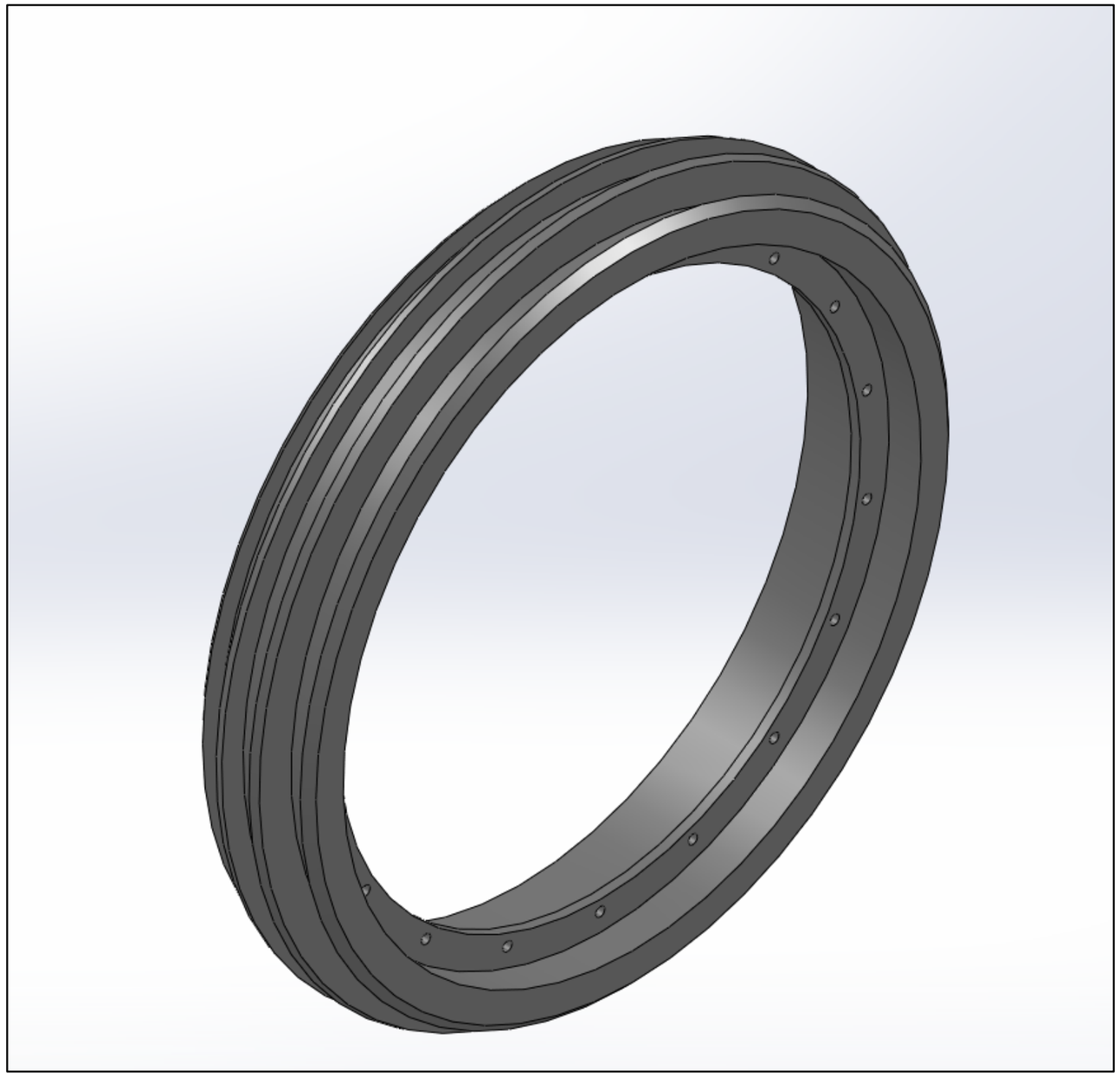

Appendix 18 – Nylon Rim for BLDC Hub Motor Solid Works Model – (Modelled By David Healy).